

## **A Cellular Automaton Model of Cancerous Growth**

AN-SHEN QI, XIANG ZHENG, CHAN-YING DU AND BAO-SHENG AN

*Department of Physics, Beijing Normal University, P.R. China*

*(Received on 15 April 1991, Accepted in revised form on 22 July 1992)*

A cellular automaton model describing immune system surveillance against cancer is furnished. In formulating the model, we have taken into account the microscopic mechanisms of cancerous growth, such as the proliferation of cancer cells, the cytotoxic behaviors of the immune system, the mechanical pressure inside the tumor and so forth. The model may describe the Gompertz growth of a cancer. The results are in agreement with experimental observations. The influences of the proliferation rate of cancer cells, the cytotoxic rate and other relevant factors affecting the Gompertz growth are studied.

### **1. Introduction**

The Gompertz model is usually employed to describe cancerous growth. Its algebraic form is given by (Steel, 1977):

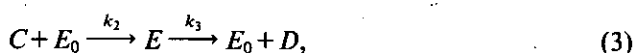
$$V = V_0 \exp \left\{ \frac{A}{B} (1 - \exp(-Bt)) \right\} \quad (1)$$

where  $V$  denotes the volume of a cancer,  $A$  and  $B$  are parameters,  $t$  represents the time variable and  $V_0$  is the initial volume. The parameters can be evaluated according to the experimental data using the method of least squares. Practically, the cancer growth described by (1) can be directly characterized by  $V_0$ ,  $A$  and  $B$ . The formula is simple and useful. However, it is purely phenomenological, namely, it does not reflect any microscopic mechanisms of cancerous growth. This situation motivated the authors to make the present cellular automaton model. The rules concern the proliferating process of cancer cells, the supply of nutrients, the behaviors of the immune surveillance system against cancer, the escaping or dissolving of dead cancer cells, the mechanical pressure inside the tumor and so forth. Thus the model presented here furnishes a microscopic explanation of the Gompertz growth. The paper is arranged as follows: in section 2, the model and the operation rules of the cellular automaton are described. Section 3 gives the results and section 4 offers a brief discussion.

### **2. The Model**

The immune surveillance network is very complicated. However, its main features can be described in a relatively simple statement. First we introduce the fundamental features of cancer growth proposed by Lefever *et al.* (Lefever & Erneux, 1984). Let

the cancerous (abnormal) cells, the dead cancer cells, the effector (cytotoxic) cells (macrophages, etc) and the complexes produced by the cytotoxic process be represented by  $C$ ,  $D$ ,  $E_0$  and  $E$ , respectively. The cell-mediated immune response to cancer can be depicted by the following reactions:



Reaction (2) describes the proliferation of cancerous cells. The first reaction in (3) denotes the cytotoxic process, in which a single effector binds to one abnormal cell at a time. The second reaction of (3) depicts the dissolution of complexes. Equation (4) describes the dissolution of dead cells. The parameters are the rates of the relevant processes. It is assumed that inside the tissue studied the sum of  $E$  and  $E_0$  remains constant:

$$E + E_0 = \text{const.} \quad (5)$$

Based on eqns (2–5), a system of reaction–diffusion equations was established by Lefever *et al.* (Lefever & Erneux, 1984). The main variable is the density of cancer cells. Thus it is a local description of cancer development. In this approach, the transformation between normal state and cancerous state of the tissue can be compared with a phase transition in physics. The important results obtained from this model are wave fronts which describe the continuous growth or regression of a malignant tumor (Lefever & Erneux, 1984; Qi, 1988). Equations (2–5) are also considered in the founding of the present model. Additionally, the restriction of nutrients for cellular replication, the mechanical pressure inside the tumor and some other factors affecting the cancer expansion are also taken into account. Different from the reaction–diffusion approach mentioned above, the modeling presented here deals with the time evolution of the cancer as a whole. Thus we obtain a global description of the cancer development.

Now consider a square lattice of two dimensions which is divided into  $n \times n$  equal sites or compartments. Each compartment has four nearest neighborhoods. A site or a compartment is symbolized by  $(i, j)$ . Each site may accommodate either a normal cell, a cancerous cell, a complex, or a dead cancer cell. The initial configuration is arranged as follows: At  $t=0$ , only five cancer cells are set in the central part of the square lattice and all of the remaining sites are occupied by normal cells [Fig. 1(a)]. Moreover, one imagines that there is an effector cell hiding in each compartment. The time step size is “1 day”. From  $t$  to  $t+1$ , the cellular automaton operations are applied to the sites one by one according to the following rules:

(1) If the compartment  $(i, j)$  is occupied by an abnormal cell, it may proliferate with probability  $k_1'$  or may be bound by the effector cell hiding in the same site with probability  $k_2$ .

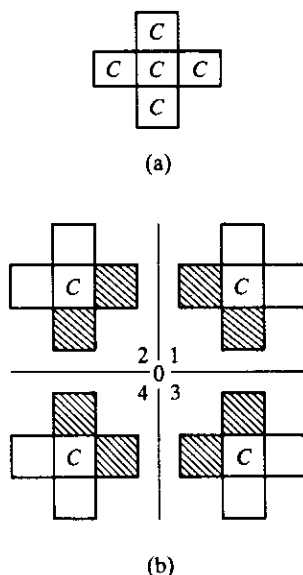


FIG. 1. (a) At  $t=0$ , five cancer cells are set at the center of the square lattice as the initial condition. (b) 0 denotes the center of the square lattice. The numbers 1, 2, 3 and 4 denote the four quadrants. The sites symbolized by  $C$  are sites to which the automaton rules are applied. The shadowed sites and the blank sites are the inside and the outside neighboring sites of " $C$ ", respectively.

Let  $k_1$  describe the proliferation rate of cancer cells *in vitro*. The cellular replication *in vitro* can acquire sufficient nutrients, thus  $k_1$  could remain constant. The cellular proliferation *in vivo*, studied in the present model, is obviously restricted by the supply of nutrients. This implies that the proliferation rate  $k'_1$  *in vivo* would decrease inevitably as the malignant tumor expands. Thus it is reasonable to assume that  $k'_1 = k_1(1 - N_c/\phi)$ , where  $N_c$  denotes the total number of cancer cells and  $\phi$  denotes a constant. Even though there is no cytotoxic behavior, as soon as  $N_c$  reaches the maximum  $\phi$  the proliferation of abnormal cells would stop owing to the lack of nutrients.

If cell  $C$  located at  $(i, j)$  may duplicate, one of its daughter cells will occupy the original position and the other will randomly invade one of the nearest neighboring sites primarily occupied by normal cells. This operation reflects the invasion of the cancerous tissue into the normal tissue. *In vivo*, there are two factors affecting the proliferation and the invasion, which are absent *in vitro*. First, the proliferation and invasion *in vivo* may proceed only if at least one of the neighboring sites is occupied by a normal cell. If all of the four neighboring sites are occupied by either  $C$ ,  $E$  or  $D$ , the proliferation is forbidden. This can be thought of as a spatial restriction on the proliferation process. Second, the mechanical pressure within the tumor is probably an important factor in local invasion (Easty, 1975). Only if the pressure inside the tumor is high enough, the expansion of the tumor is possible. The mechanical pressure is closely related to the density of cancerous cells. The density is introduced

as follows. Let  $N_E$  and  $N_D$  denote the number of complexes and dead cancer cells, respectively. Also define  $N = N_c + N_E + N_D$ . First we take the center of the square lattice as the co-ordinate origin and define the average radius of the malignant cell distribution as  $R = (\sum R_{ij})/N$ , where  $R_{ij}$  depicts the distance from the compartment  $(i, j)$  occupied by a cancer cell and the origin. The density of cancer cells is defined as  $d = N/(R^2)$ . The purpose of introducing  $d$  is to describe the effect of the mechanical pressure on cancer development. Considering these two factors, one replenishes the following rule: a critical value of  $d$ ,  $d = d_c$  is chosen. If  $d \leq d_c$ , the second daughter cell resulting from the proliferation can only occupy one of the inside nearest neighboring sites originally occupied by normal cells with the same probability [Fig. 1(b)]. If  $d > d_c$ , the second daughter cell may invade any one of the nearest neighboring sites originally occupied by normal cells with the same probability.

If the cancer cell located at  $(i, j)$  can not proliferate and is bound by an effector, the cancer cell disappears and a complex occupies the same compartment.

(2) If the compartment is occupied by a complex, it may dissolve with probability  $k_3$ . If it dissolves, the complex is replaced by a dead cancer cell and we should imagine that an effector cell  $E_0$  goes into hiding in the same compartment.

(3) If a dead cell occupies  $(i, j)$ , it may escape or dissolve with probability  $k_4$ , if it escapes or dissolves, the compartment will be occupied by a normal cell accompanied with a hiding effector cell. This operation represents the infiltration of the normal tissue into the cancerous tissue.

The values adopted for the parameters  $k_1$ ,  $k_2$ ,  $k_3$  and  $k_4$  are listed in Table 1. To overcome the lack of the experimental data for  $k_4$ , the value of  $k_4$  is considered to vary over a wide range ( $0.1-0.4 d^{-1}$ ). The numbers  $n$ ,  $\phi$  and  $d_c$  have biological meanings as mentioned above. But their evaluations are limited by the computer simulations. For instance, although a real tumor contains billions upon billions of cells, the square lattice on the computer screen can accommodate many fewer cells. Suppose one chooses  $n = 101$ . This implies that the square lattice can only accommodate about  $10^4$  cells. Suppose further that  $\phi = 10^3$ . This choice guarantees that the "developing cancer" does not touch the border of the square lattice, so the border

TABLE 1

*Values adopted for parameters  $k_1$ ,  $k_2$ ,  $k_3$  and  $k_4$*

Parameter	Value ( $d^{-1}$ )	Type of cells
$k_1^\dagger$	0.26-0.48	Spontaneous carcinoma C3H in mice
	0.58-0.89	Mouse carcinoma KHT
$k_2^\ddagger$	0.2-0.4	Syngeneic-activated macrophages
$k_3^\ddagger$	0.2-0.65	Syngeneic-activated macrophages
$k_4$	0.1-0.4	

<sup>†</sup> The values of  $k_1$  are obtained by calculations using the data provided by Altman *et al.* (1976) and the formulas used by Bresciani *et al.* (1974). In calculations it is assumed that 60-80% of the malignant tumoral cells are in the replicating state (other cancer cells are in the resting state) (Baserga, 1985).

<sup>‡</sup> The data for  $k_2$  and  $k_3$  are taken from Garay & Lefever (1978).

does not influence the cancer growth. The evaluation of  $d_c$  gives the influence of the mechanical pressure on the cancer development. The value of  $d_c$  is chosen such that  $N_c$  and  $R$  reach their maxima simultaneously.

### 3. Results

(1) Comparisons between theoretical results and experimental observations: The model's behavior can be displayed on a computer screen. The shape of the tumor is shown in Fig. 2. With definite values of the parameters, we obtain the curves of  $N$ ,  $N_c$  and  $R$  vs.  $t$  as shown in Fig. 3. It is seen that  $N$ ,  $N_c$  and  $R$  reach their maxima simultaneously. We find the time  $t_s$  which roughly depicts the time needed for the cancer to reach its maximum.

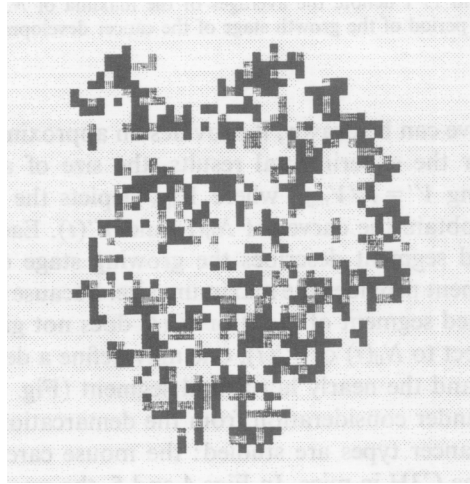


FIG. 2. The shape of a tumor.  $k_1=0.4 d^{-1}$ ,  $k_2=0.1 d^{-1}$ ,  $k_3=k_4=0.35 d^{-1}$ ,  $d_c=3.7$ ,  $\phi=10^3$  and  $t=150$ . The black, dark grey and white colors denote  $C$ ,  $E$  and  $D$ , respectively. The light grey background represents the normal tissue.

Now we will compare the theoretical results and the experimental observations. To make the comparison convenient, for the theoretical results, we introduce  $N_0 = N/N_{\max}$ , where  $N_{\max}$  denotes the maximum of  $N$ . In other words, the maximum size of the tumor is normalized to one. The experimental results are usually systematically described invoking the Gompertz formula. Based on the experimental data, the parameters  $V_0$ ,  $A$  and  $B$  in (1) are determined using the method of least squares.

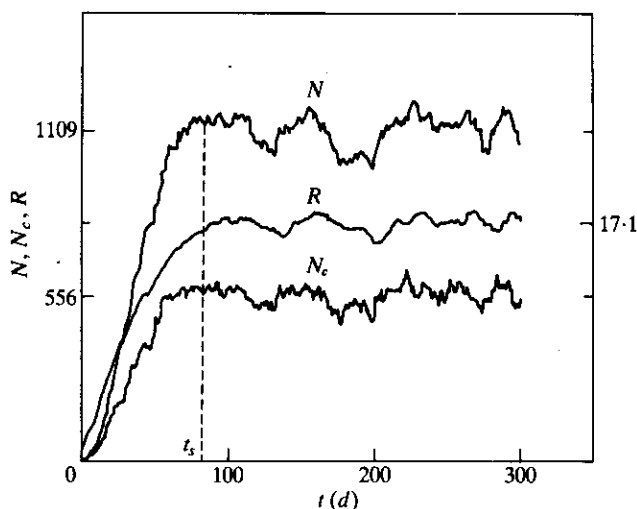


FIG. 3. The time evolutions of  $N$ ,  $N_c$  and  $R$ .  $k_1 = 0.74 \text{ d}^{-1}$ ,  $k_2 = 0.2 \text{ d}^{-1}$ ,  $k_3 = k_4 = 0.4 \text{ d}^{-1}$  and  $d_c = 3.85$ . The numbers 1109, 556 and 17.1 denote the averages of the maxima of  $N$ ,  $N_c$  and  $R$ , respectively.  $t_s$  roughly describes the time period of the growth stage of the cancer development.

Then a Gompertz curve can be drawn; it provides an approximate description of the cancer evolution. For the experimental results, the size of a tumor may also be normalized introducing  $V' = V/V_{\max}$ , where  $V_{\max}$  depicts the maximum volume of the cancer. Then we obtain the curves of  $N_0(t)$  and  $V'(t)$ . Each curve includes two segments: the inclined segment describes the growing stage of the tumor and the nearly horizontal segment provides the maximum size. Because the size is normalized, the slope of the inclined segment of  $N_0(t)$  or  $V'(t)$  does not give the growth rate of the cancer. With respect to  $N_0(t)$  or  $V'(t)$ , one may define a demarcation  $A$  between the inclined segment and the nearly horizontal segment (Fig. 4). We may also find the  $t_s$  for the cancer under consideration from the demarcation.

In this note, two cancer types are studied: the mouse carcinoma KHT and the spontaneous carcinoma C3H in mice. In Figs 4 and 5, the smooth curves denote the Gompertz approaches and the trembling curves denote the results provided by the present model. The agreement is clearly acceptable. It is seen from the figures that the time period  $t_s$  of the spontaneous carcinoma C3H in mice is longer than that of the mouse carcinoma KHT.

Figure 5(a) and (b) show spontaneous carcinoma C3H in mice. In these two figures the values for  $A$  are the same, as well as the values for  $B$ . However, the values of  $k_1$  and  $k_2$  in Fig. 5(a) are bigger than those in Fig. 5(b). We see that the curves in these two figures are quite similar. This situation implies that even if different growing cancers exhibit quite similar macroscopic evolutions of  $N_0$ , their detailed microscopic processes may not be the same. This result is reasonable and is roughly explained as follows. There are several microscopic factors affecting the tumor development. The values of  $k_1$  and  $k_2$  in Fig. 5(a) are bigger than those in Fig. 5(b). The increase of  $k_1$

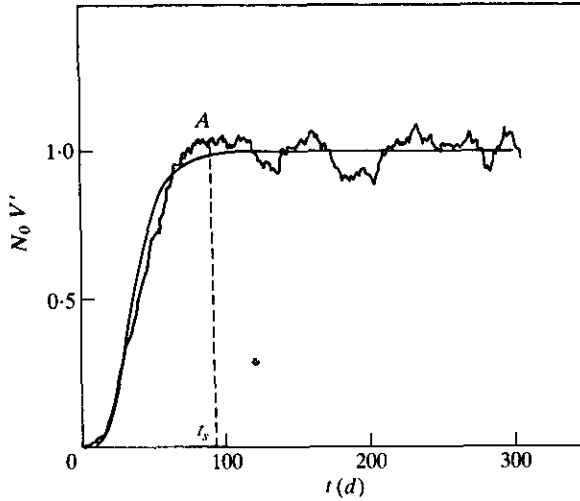


FIG. 4. The comparison between the theoretical prediction and the Gompertz approach for the mouse carcinoma KHT. The parameters of the model are:  $k_1=0.74 \text{ d}^{-1}$ ,  $k_2=0.2 \text{ d}^{-1}$ ,  $k_3=k_4=0.4 \text{ d}^{-1}$  and  $d_c=3.85$ . The Gompertz parameters are:  $V_0=1.03 \times 10^{-4} \text{ cm}^3$ ,  $V_{\max}=32.6 \text{ cm}^3$ ,  $A=0.997 \text{ d}^{-1}$  and  $B=0.0787 \text{ d}^{-1}$  (Steel, 1977).

accelerates the growth of the tumor. However, the increase of  $k_2$  makes the cancer regress more rapidly. The effects of these two factors cancel each other out. Then we may conclude that different microscopic processes possibly support the same phenomenological Gompertz evolution  $N_0(t)$ . It is worth paying attention to the fact that for the cases shown in Fig. 5(a) and (b) the evolutions of the non-normalized  $N$  are not similar [Fig. 5(c)]. On the other hand, it should be pointed out that if the parameter values (such as  $k_1$ ,  $k_2$ ,  $k_3$ ,  $k_4$ , etc are given and a Gompertz growth is obtained, we always obtain quite similar Gompertz evolutions. Thus we expect that if the parameters  $k_1, \dots, k_4$  could be measured from experiments, one may estimate the cancer development of the Gompertz type.

(2) The influences of parameters on the Gompertz growth: the influences of  $k_1$ ,  $k_2$ ,  $k_3$  and  $k_4$  on Gompertz growth are now investigated. In this subsection,  $N$ ,  $N_c$  and  $R$  (without normalization) are chosen to measure the size of a tumor.

Figure 6(a) shows the influence of  $k_1$  on the growth rate of a tumor. The growth rates of  $N$  and  $N_c$  increase with  $k_1$ . It can be seen from Fig. 6(b) that the increase of  $k_2$  apparently damps the growth of the tumor, since the immune network plays a critical role in restraining a cancer. From Fig. 6(a) [or (b)], we find that the smaller the  $k_3$  (or  $k_4$ ), the slower the development of  $N_c$ . This is because the occupation of the sites by  $E$  (or  $D$ ) prevents the cancer cells from proliferating. If  $k_3$  (or  $k_4$ ) is smaller, more complexes  $E$  (or dead cancer cells  $D$ ) stay inside the tumor. Thus we find from Fig. 6(c) and (d) that the smaller the value of  $k_3$  (or  $k_4$ ), the faster the development of  $N (= N_c + N_E + N_D)$ .

Figure 7 demonstrates the influences of  $k_1$ ,  $k_2$ ,  $k_3$  and  $k_4$  on the maxima of  $N$ ,  $N_c$  and  $R$ . Figure 7(a) shows that  $N_{\max}$ ,  $N_{c\max}$  and  $R_{\max}$  increase with  $k_1$ . Figure 7(b)

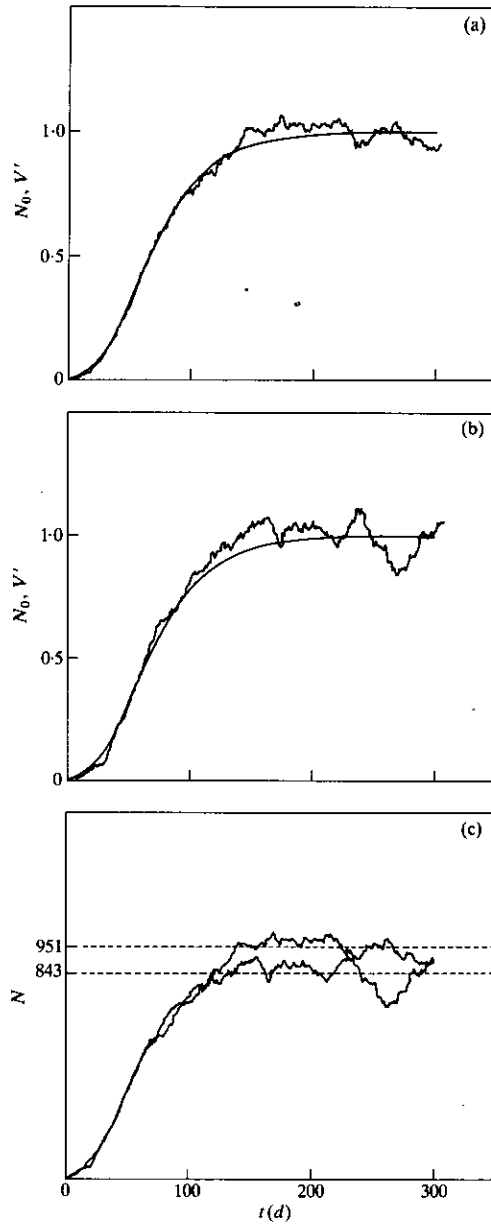


FIG. 5. The comparisons between the theoretical results and the Gompertz approaches for the spontaneous carcinoma C3H in mice. The parameters of the model are: (a)  $k_1=0.4 d^{-1}$ ,  $k_2=0.15 d^{-1}$ ,  $k_3=k_4=0.35 d^{-1}$  and  $d_c=3.45$ ; (b)  $k_1=0.35 d^{-1}$ ,  $k_2=0.1 d^{-1}$ ,  $k_3=k_4=0.35 d^{-1}$  and  $d_c=3.55$ . For both (a) and (b),  $V_0=3.76 \times 10^{-2} \text{ cm}^3$ ,  $V_{\max}=11.2 \text{ cm}^3$ ,  $A=0.177 d^{-1}$  and  $B=0.0311 d^{-1}$  (Steel 1977). (c) For the upper curve,  $k_1=0.4 d^{-1}$ ,  $k_2=0.15 d^{-1}$ . For the lower curve,  $k_1=0.35 d^{-1}$ ,  $k_2=0.1 d^{-1}$ . For both curves,  $k_3=k_4=0.35 d^{-1}$ . The numbers 951 and 843 describe the averages of  $N_{\max}$  for the two cases.



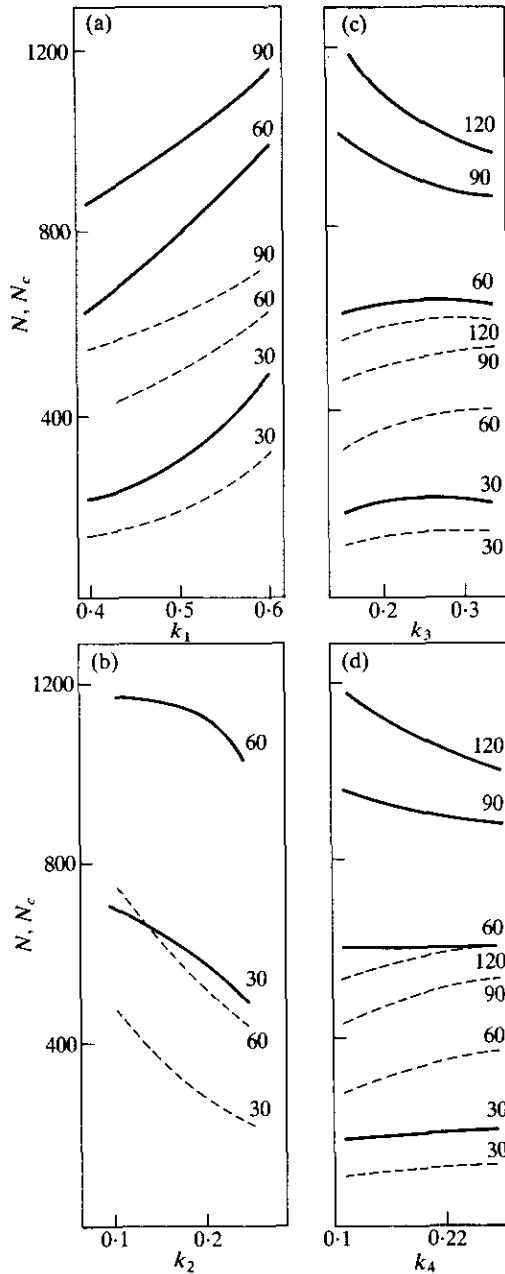


FIG. 6. The influences of (a)  $k_1$ , (b)  $k_2$ , (c)  $k_3$  and (d)  $k_4$  on the growth rate of a cancer. The real curves and the dotted curves describe the time evolutions of  $N$  and  $N_c$ , respectively. The numbers 30, 60, 90 and 120 denote the dates. In each figure, the value of  $d_c$  may change as the relevant parameter increases. In (a), for  $k_1 = 0.4 \text{ d}^{-1}$ ,  $0.5 \text{ d}^{-1}$ ,  $0.65 \text{ d}^{-1}$ , we set  $d_c = 3.7$ ,  $3.8$  and  $3.95$ , respectively; in (b) for  $k_2 = 0.1 \text{ d}^{-1}$ ,  $0.15 \text{ d}^{-1}$  and  $0.20 \text{ d}^{-1}$ , we set  $d_c = 4.1$ ,  $4.0$  and  $3.9$ , respectively; in (c),  $d_c = 3.7$  and in (d),  $d_c = 3.8$ . For (a)  $k_2 = 0.1$ ,  $k_3 = 0.35$ ,  $k_4 = 0.35$ ; (b)  $k_1 = 0.8$ ,  $k_3 = 0.35$ ,  $k_4 = 0.35$ ; (c)  $k_1 = 0.4$ ,  $k_2 = 0.1$ ,  $k_4 = 0.35$ ; (d)  $k_1 = 0.4$ ,  $k_2 = 0.1$ ,  $k_3 = 0.35$ .

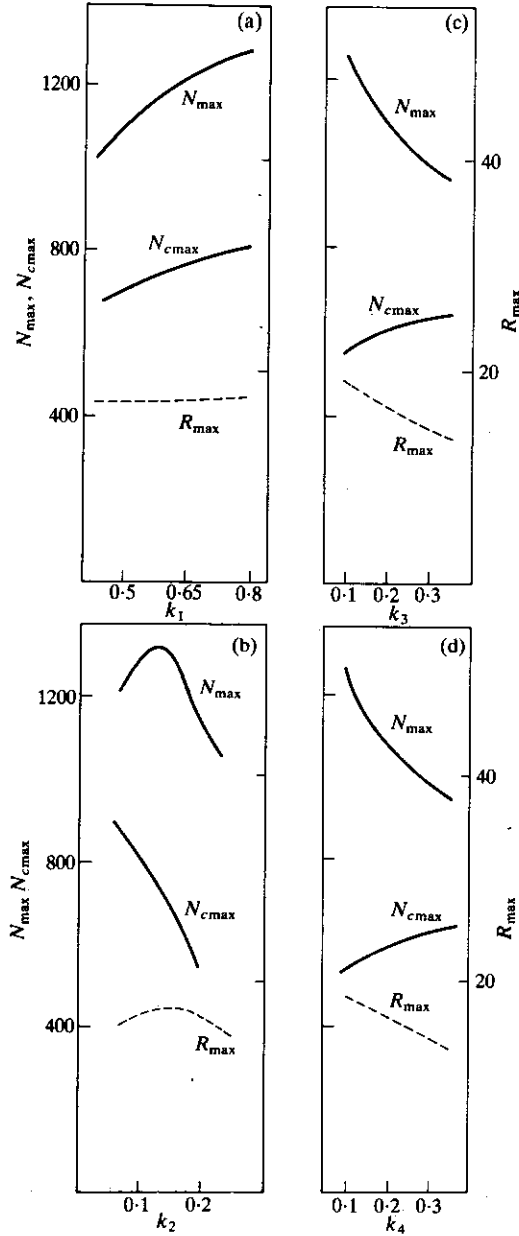


FIG. 7. The influences of the parameters (a)  $k_1$ , (b)  $k_2$ , (c)  $k_3$  and (d)  $k_4$  on the maxima of  $N_{\max}$ ,  $N_{c\max}$  and  $R_{\max}$ .  $N_{\max}$ ,  $N_{c\max}$  and  $R_{\max}$  are averages taken over 100–250 days after the tumor arrives at its maximum. For (a)  $k_2 = 0.1$ ,  $k_3 = 0.35$ ,  $k_4 = 0.35$ ; (b)  $k_1 = 0.8$ ,  $k_3 = 0.35$ ,  $k_4 = 0.35$ ; (c)  $k_1 = 0.4$ ,  $k_2 = 0.1$ ,  $k_4 = 0.35$ ; (d)  $k_1 = 0.4$ ,  $k_2 = 0.1$ ,  $k_3 = 0.35$ .

shows the effects of  $k_2$  on  $N_{\max}$ ,  $N_{c\max}$  and  $R_{\max}$ . Here, more cancer cells are killed as  $k_2$  increases. Therefore  $N_{c\max}$  decreases as  $k_2$  increases. It is interesting that the curves of  $N_{\max}$  vs.  $k_2$  and  $R_{\max}$  vs.  $k_2$  have maxima. We explain this in what follows.  $N$  consists of three components:  $N_c$ ,  $E$  and  $D$ . Each of them is affected by  $k_2$ . Thus  $N_{\max}$  exhibits complicated behavior. The influences of  $k_3$  and  $k_4$  on the maximum size are demonstrated in Fig. 7(c) and (d). The shapes of the curves in these two figures are similar. Consider Fig. 7(d). When  $k_4$  increases, more dead cancer cells disappear and  $N_{\max}$  decreases. On the other hand, the disappearance of dead cancer cells produces empty sites for the cancer cells to proliferate. Thus  $N_{c\max}$  increases with  $k_4$ .

According to the above discussion, we see that  $N$ ,  $N_c$  and  $R$  may demonstrate different behaviors. We further see that large tumors do not necessarily contain a high ratio of cancer cells. Similarly, small cancers may have a high ratio of abnormal cells.

#### 4. A Brief Discussion

It can be seen that the results given by the model fit the relevant observed cancer growth curves. We hope that if the kinetic parameters ( $k_1$ , etc) could be measured, the macroscopic Gompertz development of cancer could be estimated.

We now compare the present model with the well-known Eden model. In the Eden model and in some epidemic models (Eden, 1961; Bunde *et al.*, 1987), the growth sites are generally located along the surface of the expanding pattern. The growth is naturally considered as a surface phenomenon (Herrmann, 1986). The present model is different from them. The replication of cancer cells, the cytotoxic behaviors, the dissolving of complexes and the escaping or dissolving of dead cancer cells happen not only at the surface of the cancerous tissue but also inside the tumor. This is more realistic than surface models.

It can be seen from Fig. 2 that the shape of a tumor is irregular at each lattice site, however, the operation rules of cellular automaton are the same. Thus the tumor development described by the present model possesses a fractal structure in a statistical sense. The statistical properties of a tumoral growth can be characterized by its fractal dimensions. Additionally, the model may exhibit other complex behaviors. These results will be reported in the near future.

The authors are grateful to Professor W. Alt for helpful discussions. The authors are also grateful to Professors Xue Shao-bai, Zhang Hong-qing, Mr Chu Qi-ren and Ms Wang Ai-ping for their fruitful help.

#### REFERENCES

- ALTMAN, PHILIP, L. & KATZ, D. D. (1976). *Cell Biology, Biological Handbooks*, Vol. 1. Maryland. Federation of American Societies for Experimental Biology.
- BASERGA, R. (1985). *The Biology of Cell Reproduction*. Cambridge, MA: Harvard University Press.
- BRESCIANI, F. *et al.* (1974). Cell kinetics and growth of squamous cell carcinomas in man. *Cancer Res.* **34**, 2405-2415.

- BUNDE, A. (1987). From the Eden model to kinetic growth walk: a generalized growth model with a finite lifetime of growth sites. *J. Stat. Phys.* **47**, 1-16.
- EASTY, G. C. (1975). Invasion by cancer cells. In: *Biology of Cancer* (Ambrose, E. J. & Croe, F. J., eds) p.58. Ellis Horwood Limited.
- EDEN, M. (1961). A two dimension growth process. In: *Proceedings of the Fourth Berkeley Symposium Vol. IV: Mathematical Statistics and Probability* (NeyMan, F., ed.) p.223. Berkeley, CA: University of California Press.
- GARAY, R. P. & LEFEVER, R. (1978). A kinetic approach to the immunology of cancer: stationary state properties of effector-target cell reactions. *J. theor. Biol.* **73**, 417-438.
- HERRMANN, H. J. (1986). Geometrical cluster growth models and kinetic gelation. *Phys. Reports* **136**, 153-227.
- LEFEVER, R. & ERNEUX, T. (1984). On the growth of cellular tissues under constant and fluctuating environmental conditions. In: *Nonlinear Electrodynamics in Biological Systems* (Ross, W. & Lawrence, A, eds) p.287. Plenum Publishing Corporation, New York.
- QI, A.-S. (1988). Multiple solutions of a model describing cancerous growth. *Bull. math. Biol.* **50**, 1.
- STEEL, G. G. (1977). *Growth Kinetics of Tumors*. Oxford: Clarendon Press.